American Mineralogist, Volume 83, pages 23–35, 1998

Thermoelastic properties of $MgSiO_3$ perovskite using the Debye approach

ORSON L. ANDERSON

Center for Physics and Chemistry of Planets, Institute of Geophysics and Planetary Physics, Department of Earth and Space Sciences, University of California at Los Angeles, Los Angeles, California 90095-1567, U.S.A.

ABSTRACT

$MgSiO_3$ perovskite is shown to be a Debye-like mineral by the determination of specific heat, C_V, entropy, S, and thermal pressure, ΔP_{Th}, using the Debye theory up to 1800 K. Sound velocities and bulk moduli at ambient conditions published by Yeganeh-Haeri were used to find the ambient acoustic Debye temperature, Θ_D^{ac}. The variation of Θ_D^{ac} with T was assumed to be a curve parallel to the Θ_D^{ac} vs. T curves previously found for Al_2O_3, MgO, and $MgSiO_3$, enabling $\Theta_D^{ac}(T)$ to be given up to 1800 K. To determine C_P, the thermal expansivity, α, and the isothermal bulk modulus, K_T, are needed. After considering several sets of $\alpha(T)$, the $\alpha(T)$ data of Funamori and his colleagues were chosen. Using the ambient K_T and the values of $(\partial K_T/\partial T)_P$ vs. T reported by Jackson and Rigden, $K_T(T)$ up to 1800 K was found. Then $C_P(T)$ up to 1800 K was found assuming quasiharmonicity in C_V. The data behind the $C_P(T)$ calculation are also sufficient to find the Grüneisen parameter, $\gamma(T)$, and the Anderson-Grüneisen parameters, δ_T and δ_S, up to 1800 K. The value of $q = (\partial \ln \gamma/\partial \ln V)_T$ was found, and with γ and ρ, ΔP_{Th} vs. V and T was determined. The three sound velocities, v_s, v_p, and $v_b = \sqrt{K_S/\rho}$, were then determined to 1800 K. From v_s and v_p, Poisson's ratio and the isotropic shear modulus, G, were found to 1800 K. $MgSiO_3$ perovskite is one of a small, select group of Debye-like minerals for which thermoelastic properties and the equation of state (EOS) are calculable from acoustic data.

INTRODUCTORY REMARKS ON DEBYE THEORY

Thermoelastic properties for a Debye solid, such as C_p vs. T, at $P = 0$ can be easily calculated from standard Debye tables. A Debye solid is a monatomic solid (typically a metal) in which thermoelastic properties are a function of only one characteristic frequency, ω_D, which is equivalent to one characteristic temperature, Θ_D (Debye 1912). The specific heat, C_V, of a Debye solid is defined as (Kittel 1971)

$$C_V = 3R\mathcal{D}\left(\frac{\Theta_D}{T}\right) \tag{1}$$

where Θ_D is the Debye temperature; R is the gas constant; and $\mathcal{D}(\Theta_D/T)$ is the Debye function for specific heat found from tables. Most solids of interest to geoscience are not monatomic. Debye theory may be applied usefully to certain polyatomic minerals, provided the vibrational phonon density of states is well approximated by a Debye frequency spectrum (Kittel 1971),

$$\begin{aligned} g(\omega) &= a\omega^2 \qquad \omega \le \omega_D \\ &= 0 \qquad\quad \omega > \omega_D \end{aligned} \tag{2}$$

where ω_D corresponds to Θ_D.

Equation 2 does not work as a substitute for the phonon density of states if the solid has a wide band gap, as found in NaI, α-quartz, or calcite. Polyatomic solids in which Equation 2 is a useful substitute for the phonon density of states are called Debye-like solids; these include NaCl, MgO, Al_2O_3, and, as we shall see, $MgSiO_3$ perovskite. Minerals are rarely Debye-like solids because their thermoelastic properties are not usually a function of a single characteristic temperature. Note that there is no consideration of optic modes in a Debye-like solid.

The pertinent parameters are v_s and v_p, the shear and longitudinal sound velocities, and the maximum phonon frequency, ω_D (or temperature, Θ_D). The value of Θ_D is found from the sound velocities as given by the relation between Θ_D and the mean sound velocity, v_m (Poirier 1991)

$$\Theta_D = 251.2\left(\frac{\rho}{\mu}\right)^{1/3} v_m \tag{3}$$

where $\mu = M/p$ is the mean atomic mass; M is the molecular mass; p is the number of atoms in the vibrating cell ($p = 2$ for NaCl or MgO); and ρ is the density. v_m, the mean sound velocity, is related to the measured sound velocities by

$$\frac{3}{v_m^3} = \frac{2}{v_s^3} + \frac{1}{v_p^3}. \tag{4}$$

v_m is only slightly larger than v_s, as seen when Equation 4 is written as

$$v_m = v_s\left\{\frac{3}{2 + (v_s/v_p)^3}\right\}^{1/3} \tag{5}$$

0003–004X/98/0102–0023$05.00

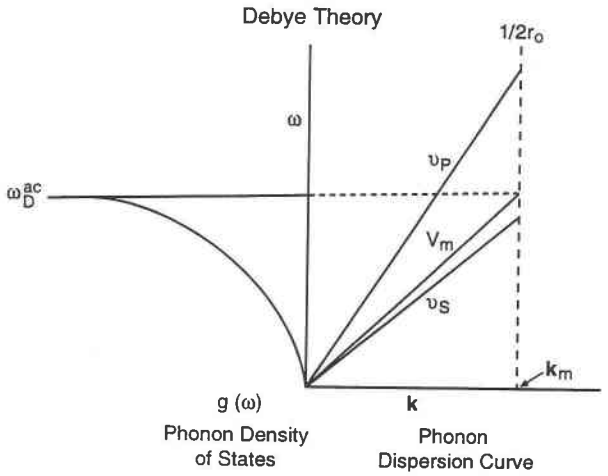

FIGURE 1. The phonon dispersion curve, ω vs. **k**, for a Debye solid that terminates at the maximum, $1/2r_o$. Under the assumptions of isotropy, there are two acoustic branches in a Debye solid, the upper one having a slope of v_p in kilometers per second and the lower one having a slope of v_s in kilometers per second. Debye theory requires an acoustic branch with the mean slope v_m, Equation 4. To the left are the phonon density of states, g(ω), vs. ω, where the maximum frequency or Debye frequency, ω_D^{ac}, is pinned to the maximum wave number, $\mathbf{k}_m$, at v_m.

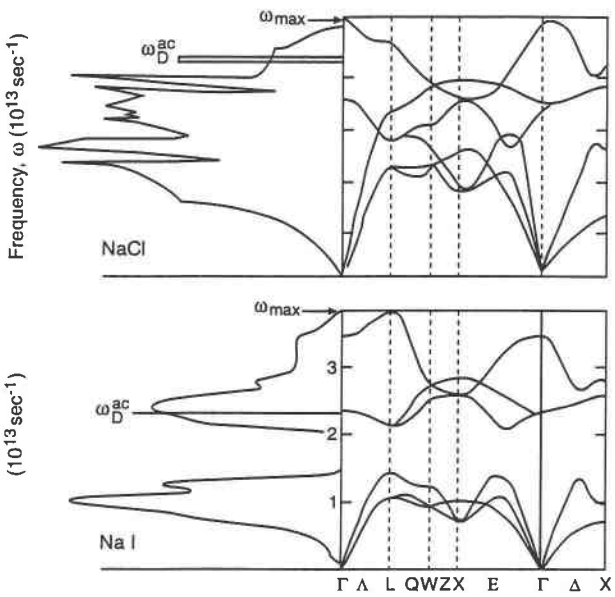

FIGURE 2. Three-dimensional phonon dispersion curves and the resulting density of states curves. (Top) NaCl showing the dispersion curves to the right and the phonon density of states to the left. The Debye frequency, ω_D^{ac}, given by measured velocities of sound, is labeled as the line at the top. This shows that most values of ω are less than ω_D^{ac}; hence NaCl is a Debye-like solid. (Bottom) NaI has a big band gap in ω near the center of the spectrum. The line labeled ω_D^{ac} is near the center of the density of states, and there are many modes whose frequency, ω, is larger than ω_D^{ac}. Hence NaI is not a Debye-like solid (modified from Birman 1984).

(Anderson 1995). For typical ratios of (v_s/v_p), say 0.6, $v_m = 1.11\ v_s$. The acoustic frequencies are terminated at a wave number **k** that is the reciprocal of the smallest interatomic spacing. In acoustic branches of the frequency dispersion curves, the slope of the ω-**k** curve is the sound velocity.

These brief excerpts from Debye's theory emphasize that: (1) in this simple theory, there is no optic mode information; (2) the primary experimental information needed to apply the theory is the sound velocity (usually measured by an acoustic experiment); (3) the Debye theory applies to any temperature, provided the sound velocities and density are known at that temperature; and (4) the Debye temperature can be easily calculated from the acoustic sound velocities (Anderson 1963). For a Debye solid, the phonon-dispersion curve (a straight line), the frequency distribution (called the phonon density of states), and their relationship to each other are shown in Figure 1.

DEBYE THEORY FOR POLYATOMIC SOLIDS

For polyatomic solids, $p > 1$ and the original Debye assumptions are violated; hence the name Debye-like solids, when Equation 1 is empirically obeyed. NaCl is a good example of a Debye-like solid. The value of Θ_D determined from acoustics is 316 K at low temperature, whereas the estimate of Θ_D determined from calorimetric properties at high T is 321 K (Barron et al. 1980). The closeness in these values satisfies a requirement of Debye theory. The ω-**k** dispersion curve calculated from lattice dynamics and the resulting $f(\omega)$ curve for NaCl are plotted in Figure 2 (top), where the maximum lattice frequency is ω_{max}. Also shown is the position of ω_D from acoustics, called ω_D^{ac}, which is close to ω_{max} for NaCl.

The Debye frequency spectrum, $f(\omega)$, is a parabola (Eq. 2) terminating at ω_D^{ac} found from the experimentally determined v_m with an ordinate such that the area under the Debye curve is equal to the area under the actual phonon distribution curve, 3pN. When the value of ω_D^{ac} is close to that of the phonon dispersion determination of ω_{max}, as shown in the top of Figure 2, the thermal properties calculated by Debye theory are close in value to corresponding measured values or to those calculated from the detailed phonon density of states.

NaI is an example of a solid that is not Debye-like. NaI has a wide band gap, and the frequency cutoff, ω_{max}, is considerably larger than ω_D^{ac} calculated from the acoustic properties, as shown in Figure 2 (bottom). The phonon density of states shows that almost half the modes have frequencies higher than ω_D^{ac}. As a consequence, the specific heat curve, C_V, of NaI approaches the Dulong and Petit limit at much higher temperatures than predicted by the Debye theory.

Lattice dynamics deals with the vibrations of the whole lattice, three times Avogadro's number of vibrations. In this approach, the thermal energy is defined in a statistical sense (Born 1915, 1923; Barron 1955), and the thermoelastic properties are defined in terms of the lattice dynam-

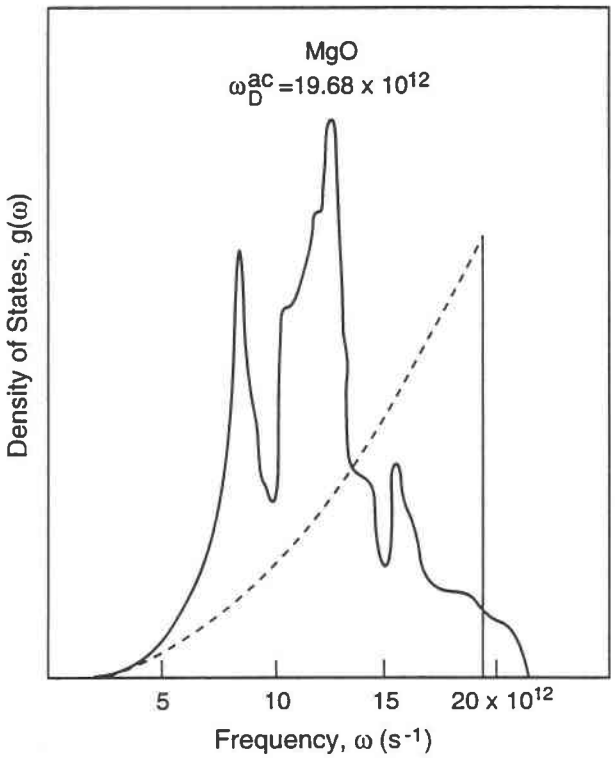

FIGURE 3. The Debye spectrum and the density of states for MgO. This solid is Debye-like because only a few frequencies are larger than ω_D^{ac}, and the two spectra merge at low frequency. Density of states is from Sangster et al. (1970).

ical phonon density of states. A fairly good approximation to the phonon density of states can be represented by a histogram of cells using data constructed mainly from measured optic modes (Kieffer 1982, 1985). I call this the Kieffer method; it is really the crystallographic approach because it deals with the individual atoms in the crystallographic cell as the central basis for computing thermal energy of vibration. Each atom gives rise to three modes of vibration that are, in principle, identifiable by a spectroscopic measurement. In a few cases, the density of states can be effectively represented by a crude approximation, called the Debye spectrum, a quadratic curve with a sharp cutoff.

In contrast to the Kieffer method, the Debye theory assumes that all modes can be approximated by two different acoustic modes only, each having no dispersion, thus ignoring the optic modes. This assumption works for a few dense polyatomic solids in which almost all the optic modes have frequencies less than ω_D^{ac}; that is, if the optic modes are confined to the interior of the phonon density of states. For polyatomic solids in which many optic modal frequencies are large in comparison with ω_D^{ac}, the Kieffer method is most useful.

In brief, a Debye-like solid is one in which the Debye spectrum maximum frequency, ω_D^{ac}, as determined by the measured sound velocity, exceeds in value most of the optic frequencies in the phonon density of states.

TABLE 1. MgO: Comparison of C_V from Debye theory with C_V calculated by the measured C_P

T (K)	Θ_D^{ac}* (K)	Θ_D^{ac}/T	C_V† Debye table [cal/(mol·K)]	C_V‡ Debye [J/(mol·K)]	C_V§ from C_P [J/(mol·K)]	C_V# density of states [J/(mol·K)]
0	940‖					
400	937	2.343	4.397	36.820	42.274	41.590
500	928	1.856	5.045	42.247	42.234	44.491
600	920	1.533	5.311	44.474	45.880	46.023
700	911	1.301	5.480	45.889	46.466	47.030
800	902	1.128	5.594	46.844	46.990	47.675
900	894	0.993	5.673	47.506	47.350	48.118
1000	885	0.885	5.729	47.915	47.550	48.100
1100	875	0.796	5.772	48.334	47.750	48.682
1200	866	0.722	5.804	48.602	47.876	
1300	857	0.659	5.829	48.812	47.957	
1400	847	0.605	5.855	49.030	47.997	
1500	838	0.559	5.864	49.105	47.997	
1600	828	0.518	5.877	49.213	48.087	
1700	820	0.482	5.888	51.143	48.077	

*Θ_D^{ac} from Table 30, Anderson and Isaak (1995).
†C_V (Debye table) from Table A–6.1, Anderson (1995): a monatomic solid ($p = 1$).
‡C_V (Debye table) for a diatomic solid ($p = 2$).
§C_V (from C_P) from Table 15, Anderson and Isaak (1995).
#C_V (from phonon density of states) from Table 2, Chopelas (1990).
‖Value of Θ_D^{ac} reported by White and Anderson (1966), who also found $\Theta_D^{cal} = 940$ K from lower temperature ($T < 30$ K) thermal expansivity.

MgO: A DEBYE-LIKE SOLID

The case of MgO illustrates a Debye-like solid. Figure 3 shows the MgO phonon density of states (Sangster et al. 1970). On this plot is placed the Debye frequency, ω_D^{ac}, determined by v_m (v_m having been determined by the isotropic averages of both v_p and v_s). It is seen in Figure 3 that for the phonon density of states, the bulk of the optic modes is at frequencies between the high peak at 13×10^{12} s^{-1} and ω_D^{ac}, and only a small tail of frequencies exceeds ω_D^{ac} (19.68×10^{12} s^{-1}).

At absolute zero, Θ_D^{ac} should be equal to the thermally determined Debye temperature, Θ_D^{th}, at $T = 0$ (Barron 1957). This is indeed the case for MgO. White and Anderson (1966) reported that at absolute zero, $\Theta_D^{ac} = 940$ K, whereas $\Theta_D^{th} = 946$ K. Also Barron (1957) showed that for a Debye solid Θ_D^{ac} and Θ_D^{cal} should be equal at high temperature. For MgO, Θ_D^{ac} at 1200 K is 866 K, and Barron (1977) reported from his study of Debye-Waller factors that the calorimetric Θ at infinite temperature ($T > \Theta$) is near 810 K.

A crucial test for the existence of a Debye-like solid is to calculate C_V from the Debye theory, then compare it with C_V computed from the measured C_P, as done in Table 1 for MgO. Data on C_V from C_p from 400 to 1700 K in the table are taken from Table 15 in Anderson and Isaak (1995). C_V computed from the Debye theory, where the acoustic Θ_D^{ac} descends slowly with T, is taken from Table 30 of Anderson and Isaak (1995). In this table we see that C_V from measured C_p differs from C_V calculated from

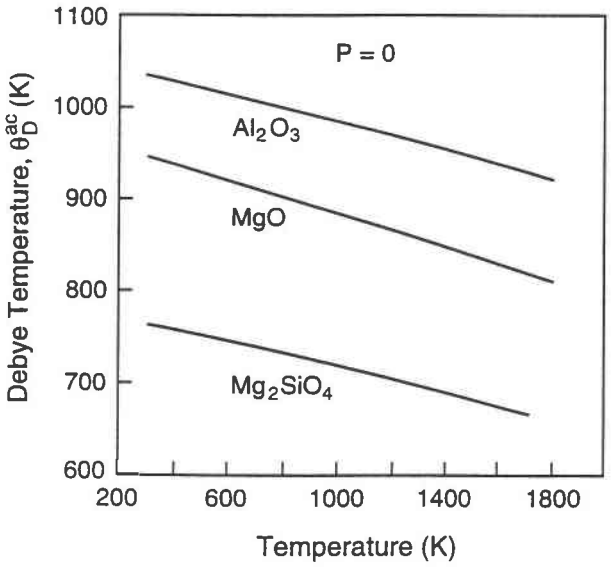

FIGURE 4. Debye temperature, Θ_D^{ac}, vs. T for three oxide solids. These three plots show that Θ_D^{ac} descends slowly with T and that the lines are parallel (data from Anderson and Isaak 1995).

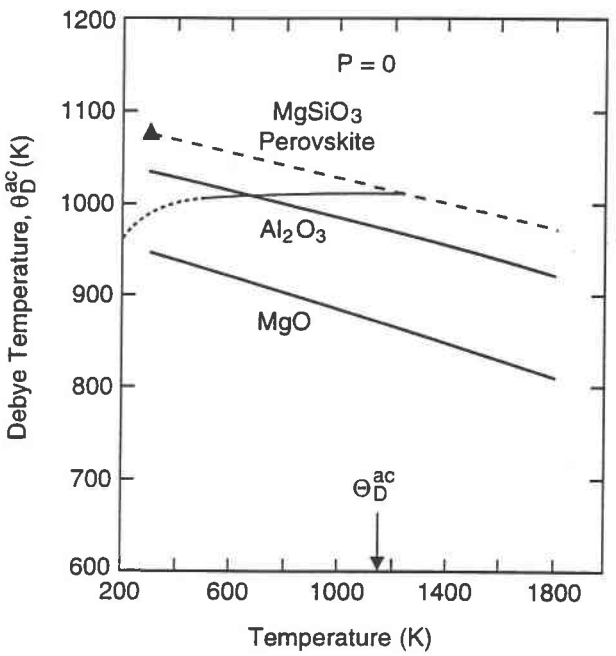

FIGURE 5. Debye temperature, Θ_D^{ac}, vs. T for $MgSiO_3$ perovskite. The value, Θ_D^{ac} = 1080 K, is anchored at T = 300 K by the acoustic experiments of Yeganeh-Haeri (1994). The Θ_D^{ac} curve is made parallel to the Al_2O_3 and MgO lines. The dotted line represents the calorimetric determination of Θ, Θ_D^{cal}, by Akaogi and Ito (1993), and their extrapolation to high T is shown by the light solid line.

acoustic velocities by less than about 2%, except for the end points.

Except for the end points, this error is within the experimental error of measured thermal expansivity, since

$$C_V = C_P - \alpha^2 K_T V T. \quad (6)$$

It is seen from Equation 6 that the conversion from C_p to C_V is sensitive to α^2, so precise determination of α is required to find the exact value of C_V from the measured C_p. Of all the variables measured in Equation 6, α is often the least well known at high T. Excepting the values at 400 and 1700 K, the agreement is within about 2%. The disagreement at 400 K arises because the Debye theory is often weakest when $T/\Theta < 0.4$. This is where the Debye C_V curve is rising rapidly with T, and a small error in T/Θ is greatly multiplied to make the uncertainty in C_V (T/Θ) large. The disagreement at 1700 K arises from the uncertainty in the measured α at that T. The overall agreement between C_V (Debye) and C_V (from C_p) is as good as can be found for most metals and is satisfactory proof that MgO is a Debye-like solid.

In the last column of Table 1 are listed the values of C_V calculated by Chopelas (1990) from the phonon density of states, as given by Sangster et al. (1970) and shown in Figure 3. The equation used to find C_V as a function of T using the phonon density of states, g(ω), is

$$C_V = 3pR \int_0^\infty \frac{e^x}{(e^x - 1)} x^2 g(\omega)\, d\omega \quad (7)$$

where $x = (h\omega)/(kT)$. The comparison between C_V as calculated by the Debye theory, C_V determined by the experimental data on C_p, and C_V from the density of states (Eq. 7), is shown in Table 1.

The main feature of the calculation of Θ_D for MgO is the steady decrease of Θ_D^{ac} with temperature resulting from the temperature dependence of the sound velocities (plotted in Fig. 4). I depart from customary procedure in that the acoustic data here appropriate to every temperature are used to determine the value of Θ_D^{ac} and in the calculation of C_V at that temperature. Also plotted in Figure 4 is Θ_D^{ac} vs. T for two other solids: Al_2O_3 and Mg_2SiO_4. Note that the slopes of Θ_{ac} vs. T are similar for all three minerals.

The assumed variation of Θ_D^{ac} with T for $MgSiO_3$ perovskite is shown in Figure 5, plotted as a dashed line. The slope of $MgSiO_3$ vs. T is made parallel to the measured slopes of Al_2O_3 and MgO. The triangle plotted in Figure 5 is from the Brillouin measurements of Yeganeh-Haeri (1994), giving v_s and v_p, which anchor the low-T end of $\Theta_D^{ac}(T)$. Using specific heat data, Akaogi and Ito (1993) estimate Θ_D^{cal} and its variation with T from 100 to 400 K, as shown by the dotted line in Figure 5. The Akaogi and Ito estimated value for Θ_D^{cal} at 1000 K is 1030 (20), agreeing well with the value for Θ_D^{ac} = 1027 K at 1000 K.

$MgSiO_3$ PEROVSKITE: ANOTHER DEBYE-LIKE SOLID

The phonon density of states of $MgSiO_3$ perovskite

The Debye theory customarily is assumed to apply to $MgSiO_3$ perovskite whenever the thermal energy factor, E_{Th}, in the Mie-Grüneisen expression for thermal pressure

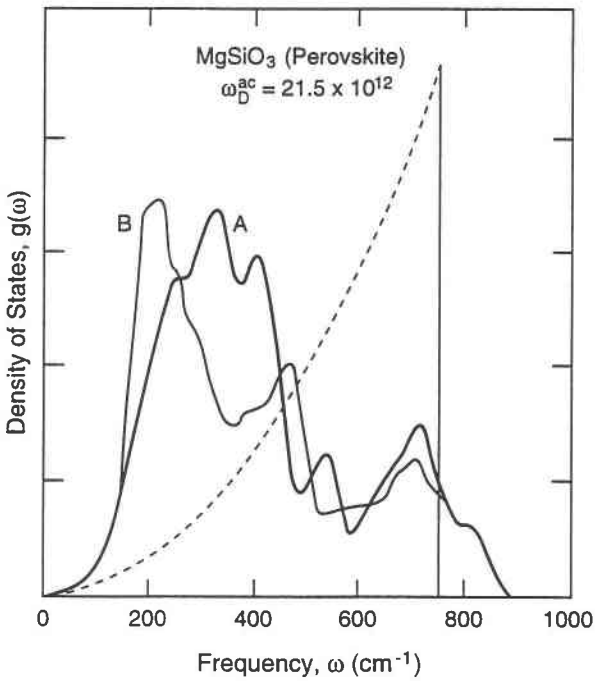

FIGURE 6. The phonon density of states for $MgSiO_3$ perovskite: (**A**) from Choudhury et al. (1988) and (**B**) from Winkler and Dove (1992). These are compared with the Debye spectrum, where $\omega_D^{ac} = (h/k)\Theta_D^{ac}$. As in the case of MgO (Fig. 3), only a small portion of the spectrum has frequencies higher than ω_D^{ac}, and the Debye spectrum and the density of states merge at low frequency. This is evidence that $MgSiO_3$ perovskite is a Debye-like solid.

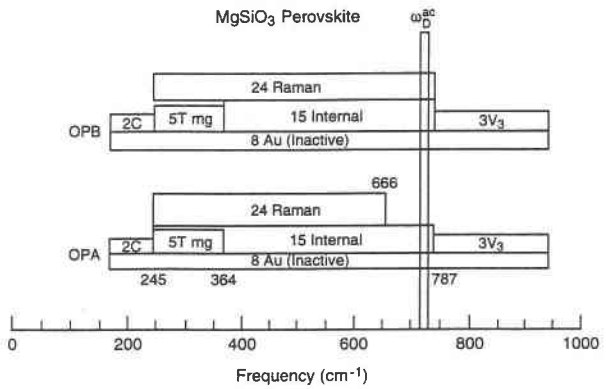

FIGURE 7. The phonon density of states for $MgSiO_3$ perovskite constructed from optic modes (the Kieffer approach) by Lu et al. (1994). Note again that the majority of the modes have frequencies less than ω_D^{ac}.

is calculated by the Debye function for internal energy (as was done by Stixrude et al. 1992 and Jackson and Rigden 1996).

Liebermann (1982) calculated successfully the bulk sound velocity, v_b, of $MgSiO_3$ perovskite by the formula, $v_b\mu^{1/2}$ = constant, which was derived by Shankland (1972) from Debye theory. The idea that $MgSiO_3$ perovskite may be a Debye-like solid is certainly not new (Anderson 1995), but it has not yet been proved.

Thus I examine evidence that $MgSiO_3$ perovskite is a Debye-like solid. The phonon density of states for $MgSiO_3$ perovskite according to two sets of calculations (Choudhury et al. 1988; Winkler and Dove 1992) is shown in Figure 6. These phonon densities of states are different. The difference does not significantly affect the Debye approximation to the phonon density of states, but it does affect the calculation of moments of the spectrum, so the moment method used to find Θ_D (Anderson 1995) is not to be used for $MgSiO_3$ perovskite.

The density of states of $MgSiO_3$ perovskite is similar to that of MgO in two important features. First, the frequencies of the phonon density of states of $MgSiO_3$ perovskite are, for the most part, less than ω_D^{ac}, with only a small tail of the spectrum lying beyond the acoustic ω_D^{ac}. Second, at low frequencies, the quadratic frequency dependence of the Debye spectrum merges into the solid's phonon density of states. Note that $MgSiO_3$ perovskite satisfies the quadratic fit at low ω about as well as does MgO. Therefore we can expect the properties of MgO arising from Debye theory to be a guide for the corresponding properties of $MgSiO_3$ perovskite.

Figure 7 shows the density of states model of $MgSiO_3$ perovskite given by Lu et al. (1994). This is a Kieffer-style density of states constructed from data on measured optic modes. This plot shows the position of ω_D^{ac} as determined by the velocity measurements of Yeganeh-Haeri (1994), which is 720 cm^{-1}. This plot shows that the preponderance of optic modes lies near the mid-region of the spectrum and that few have frequencies larger than ω_D^{ac}. This is further evidence that $MgSiO_3$ perovskite is likely to be a Debye-like solid. The results of $C_V(T)$ found by using the $\Theta_D^{ac}(T)$ curve are shown in columns 3 and 4 of Table 2.

From this table it is seen that the Debye values of C_V for $MgSiO_3$ perovskite at 300 and 1000 K are 70.66 J/(mol·K) and 118.48 J/(mol·K). The values (in the same units) at the same temperatures reported by Winkler and Dove (1992) are 85.29 and 119.97. They used Equation 7 with their phonon density of states, shown in Figure 6. This further indicates that the Debye model is fairly good for the quasiharmonic calculation of C_V, provided one focuses on temperatures above 400 K. Data on C_V of $MgSiO_3$ perovskite are sparse in the literature, because C_p apparently has not been measured above 300 K (Akaogi and Ito 1993).

Calculation of $C_p(T)$ emphasizing the importance of $\alpha(T)$

Experimental data on $C_p(T)$ of $MgSiO_3$ perovskite over a limited range of T have been presented by Akaogi and Ito (1993). Comparison of C_p with the Debye model calculations, which give C_V, requires evaluation of the α^2K_TVT correction term in Equation 6. Calculations of C_P from C_V are presented in Table 3. Note that at high T, C_P from this report is substantially lower than that reported

TABLE 2. $MgSiO_3$ perovskite: C_V and C_P

T (K)	Θ_D^{ac} (K)	C_V* Debye [cal/(mol·K)]	C_V† Debye [J/(mol·K)]	C_P‡ This Report [J/(mol·K)]	C_P§ Saxena [J/(mol·K)]	C_P# Chopelas (J/mol·K)	C_P‖ Lu et al. (J/mol·K)
300	1076	3.376	70.66	78.6**	80.3	82.7	74.9
400	1069	4.273	89.59	90.6	90.5	98.1	92.1
500	1062	4.805	100.22	101.7	107.7	107.2	103.4
600	1055	5.079	106.74	108.9	114.3	113.0	111.1
700	1048	5.339	111.20	114.1	119.5	116.9	116.9
800	1041	5.482	114.46	118.0	124.0	119.8	121.5
900	1034	5.581	116.83	120.8	127.9	122.1	125.5
1000	1027	5.653	118.48	122.9	131.4	123.9	129.1
1100	1020	5.708	119.57	124.6	134.5		132.6
1200	1013	5.749	120.33	126.1	137.3		136
1300	1006	5.781	120.94	127.5	139.9		139.4
1400	999	5.888	121.54	128.7	142.3		142.9
1500	992	5.828	122.08	129.5	144.5		146.4
1600	985	5.845	122.44	130.4	146.6		150.1
1700	978	5.859	122.57	131.5	148.5		153.8
1800	971	5.871	122.93	132.4	150.4		157.7

Note: Funamori et al. (1996) values of α and V used for correction from C_V to C_P. Comparison of calculated C_P with other authors. For value of $C_P - C_V = \alpha^2 K_T V T$, see Table 4.

*C_V (Debye) $p = 1$ from the standard Debye table.

†C_V (Debye) $p = 5$: conversion from C_V (Debye) $p = 1$ to the case of $MgSiO_3$ perovskite.

‡C_P (Debye) $p = 5$ obtained by using $C_P - C_V$ corrections listed in Table 3.

§C_P: as determined by Saxena et al. (1993) using α and V from Knittle et al. (1986).

#C_P: as determined by Chopelas et al. (1994) using a Kieffer-like density of states.

‖C_P: as determined by Lu et al. (1994) using a Kieffer-like density of states and α from Mao et al. (1991).

**C_P (experiment) at 300 K = 80.6 J/(mol·K) (Akaogi and Ito 1993).

TABLE 3. Details of calculation of $C_P - C_V$ correction

T (K)	Funamori* $\alpha \times 10^5$ (K^{-1})	Knittle† $\alpha \times 10^5$ (K^{-1})	K_T‡ (GPa)	Funamori§ V (cm³/mol)	Knittle# V (cm³/mol)	This report $C_P - C_V$ (J/mol·K)	For Knittle α $C_P - C_V$ (J/mol·K)
500	2.18	3.39	257.9	24.56	24.6	1.5	3.7
600	2.45	3.67	255.4	24.58	24.7	2.3	5.1
700	2.58	3.88	252.8	24.68	24.8	2.9	6.6
800	2.63	4.06	250.2	24.78	24.9	3.4	8.1
900	2.68	4.22	247.6	24.82	25.0	4.0	9.8
1000	2.70	4.36	244.9	24.88	25.1	4.4	11.6
1100	2.74	4.50	242.2	24.94	25.2	5.0	13.4
1200	2.83	4.63	239.5	25.04	25.4	5.8	15.4
1300	2.90	4.76	236.8	25.14	25.5	6.5	18.2
1400	2.91	4.88	234.0	25.21	25.6	7.1	19.6
1500	2.93	5.00	231.0	25.28	25.7	7.5	21.9
1600	2.94	5.12	228.5	25.36	25.9	7.9	24.4
1700	2.95	5.24	225.7	25.41	26.0	8.9	26.8
1800	3.00	5.36	223.0	25.49	26.1	9.4	29.6

Note: $C_P - C_V$ correction $= \alpha^2 K_T V T$.

*α from Anderson et al. (1996) using Funamori et al. (1996) data.

†α from Saxena et al. (1993) using Knittle et al. (1986) basic data on α.

‡K_T at 300 K from Jackson and Rigden (1996) derived from K_S at 300 K measured by Yeganeh-Haeri (1994). Dependence on T given by $(\partial K_T/\partial T)_P$ presented by Jackson and Rigden (1996).

§V from Utsumi et al. (1995) and Funamori et al. (1996).

#ΔV from Saxena et al. (1993) using Knittle et al. (1986) basic data on α and V.

by Saxena et al. (1993) and by Lu et al. (1994). The difference comes from different values of α used in the correction term, which is sensitive to α^2. This difference justifies a discussion on the appropriate values of α that should be used for $MgSiO_3$ perovskite at high T.

At the time the Saxena et al. (1993) book and the Lu et al. (1994) paper were written, the values of α for $(Mg,Fe)SiO_3$ perovskite from Knittle et al. (1986) and Mao et al. (1991) were virtually unchallenged, and so they were used by these authors.

But shortly after the publication of these two reports, many experimental papers on α of $MgSiO_3$ perovskite were published (Wang et al. 1994; Utsumi et al. 1995; Funamori et al. 1996). Masuda and Anderson (1995), using the Utsumi et al. (1995) experimental data to evaluate parameters of the Suzuki equation, found $\alpha(T)$. Jackson and Rigden (1996) reported a PVT study of the combined data of Ross and Hazen (1989), Wang et al. (1994), Utsumi et al. (1995), and Funamori et al. (1996), and they recommended values of α for $\alpha(T)$. Chopelas (1996) and Gillet et al. (1996a) found $\alpha(T)$ from their spectroscopic measurements. Anderson et al. (1996) used the Funamori et al. (1996) data on $V(T)$ for $MgSiO_3$ to find $\alpha(T)$ for $MgSiO_3$; the data are listed in Table 3, column 5. All the results for $\alpha(T)$ published by the authors listed in this paragraph essentially agree with one another, and all are substantially lower than the data presented earlier by Knittle et al. (1986) and Mao et al. (1991). These comparisons of $\alpha(T)$ are illustrated in Figure 8. The value used here (see Table 3), $\alpha = 2.58 \times 10^{-5}$ at 800 K, compares well with the Gillet et al. (1996a) value, $\alpha = 2.5 \times 10^{-5}$ at 800 K.

The evaluation of the correction term, $C_P - C_V = \alpha^2 K_T T$, is shown in Table 3, in which the values of α, K_T, and V are given in detail. It is seen from Table 3 that the correction term when using the Knittle et al. (1986) α data is three times larger at 1600 K than the correction term when using the Funamori et al. (1996) α data.

The value of K_T used in computing the correction term here (column 2, Fig. 3) is found by integrating $(\partial K_T/\partial T)_P$ vs. T as presented by Jackson and Rigden (1996). This is discussed in detail later.

The value of C_V from the Debye model is shown in column 4 of Table 2; it has reached the Dulong and Petit limit at 1800 K. Because the $C_P - C_V$ correction is known for the respective α data, one can check on whether the various C_P calculations use an underlying quasiharmonic C_V. They all do. Gillet et al. (1996a) investigated the possible presence of anharmonicity by finding the effect of temperature on the Raman spectrum of $MgSiO_3$ perovskite up to 300 K and concluded that there was no evidence of intrinsic anharmonicity strong enough to affect the equation of state, even at very high temperatures (see also Gillet 1996). I conclude, therefore, that anharmonicity need not be considered in the expression for the high-temperature C_V, and that $MgSiO_3$ perovskite is indeed quasiharmonic. Calcite, on the other hand, is a solid for which an anharmonicity component is required in the C_V analysis (Gillet et al. 1996b). The various C_V models discussed here appear to be similar, but the $C_P - C_V$ correction varies depending on the choice of $K_T(T)$ and $\alpha(T)$.

In spite of the fact that the $C_P - C_V$ correction obscures the value of C_V for the last three columns in Table 2, the Debye model appears to perform as well as the other models arising from the density of states, which use varieties of the Kieffer spectrum.

Calculation of entropy

Navrotsky (1989) used the simplest approximation for the $MgSiO_3$ perovskite density of states, a simple, one-continuum model, a rectangular box, between 225 and 900 cm^{-1}, and she found that this model led to $S = 180.9$ J/(mol·K) at 1000 K. Gillet et al. (1993) replaced Navrotsky's one-continuum model with a two-cell continuum, and from this calculated S and C_P for $MgSiO_3$ perovskite between 225 and 900 cm^{-1} (a Kieffer approach) and found 235–247 J/mol for the entropy at 1100 K. I calculated 193 J/mol at 1100 K by the Debye method (see Table 4). The Gillet et al. (1993) value of C_P was 135–136.7 J/(mol·K) at 1100 K; this should be compared with 124.6 J/(mol·K) at 1100 K shown in Table 2. Akaogi and Ito (1993) reported that by using their experimental determinations of C_P, the entropy of $MgSiO_3$ perovskite is found to be 57.2 J/mol and 185.5 J/mol at 298 and 1000 K, respectively.

I found $S(300)$ from $\int_0^{300} (C_P/T)\, dT$ for the range of T below 300 K using the C_P data of Akaogi and Ito (1993) measured between 140 and 295 K. By using a short extrapolation near absolute zero, it was found that $S(300) = 57.4 \pm 4$ J/mol for $MgSiO_3$ perovskite, close to the Akaogi and Ito (1993) result mentioned above. Thus in my calculation

$$S(T) = \int_0^T \frac{C_P}{T}\, dT = 57.4 + \int_{300}^T \frac{C_P}{T}\, dT \text{ J/mol.} \quad (8)$$

The values of $S(T)$ so calculated are shown in Table 4 under the column heading S**(Debye) and in its note ($p = 5$). The values of $S(T)$ reported here also agree well with the reports of Chopelas et al. (1994) and Lu et al. (1994), in that the Debye values are between the other two values, which were based on Kieffer-type models. Thus there is reasonable agreement between the $S(T)$ from experiment and the $S(T)$ calculated from C_P (in turn calculated from the Debye C_V). Differences in entropy have as an underlying cause the difference in thermal expansivity used in the calculation of the $C_P - C_V$ correction, as well as different approximations for the density of states.

TABLE 4. Comparison of entropy at ambient pressure calculated from the Debye model and calculations from Kieffer-like density of states for $MgSiO_3$ perovskite with vibrational modes

T (K)	Θ_D^{ac}/T	S^* Debye (J/mol)	S† Lu et al.	S‡ Chopelas et al.
150	7.233	18.3		16.6
200	5.415	30.8		30.0
250	4.320	44.1		44.2
300	3.587	57.4	51.4	58.2
400	2.673	80.9	74.9	84.3
500	2.124	102.5	96.1	107.2
600	1.758	121.7	115.0	127.3
700	1.497	138.9	131.7	145.0
800	1.301	154.4	146.7	160.9
900	1.149	168.5	160.3	175.1
1000	1.027	181.3	172.5	188.1
1100	0.927	193.1	183.8	
1200	0.844	204.0	194.2	
1300	0.774	214.1	203.8	
1400	0.714	223.6	212.7	
1500	0.661	232.5	221.1	
1600	0.616	240.9	228.4	
1700	0.575	248.9	236.3	
1800	0.539	256.4	243.3	

Note: Same as bottom of Table 3, S (Debye) $p = 1$. S (Debye) $p = 1$ from the standard Debye table.

*S (Debye) $p = 5$ conversion of S (Debye) $p = 1$ to the case of Mg_2SiO_4 perovskite.

†S Lu et al. (1994) a Kieffer-like density of states model.

‡S Chopelas et al. (1994) a Kieffer-like density of states model.

Controversies over $\alpha(T)$ and $(\partial K_T/\partial T)_P$

The low sets of $\alpha(T)$ vs. the high sets of $\alpha(T)$

The value of $\alpha(T)$ chosen from the set of $\alpha(T)$ values available for $MgSiO_3$ perovskite has a strong effect on the values of entropy and specific heat, as shown above. The choice of $\alpha(T)$ has a strong effect on the predicted density distribution of perovskite at lower mantle conditions as well (Jackson 1983; Stixrude et al. 1992).

In the upper set of values of $\alpha(T)$ found in Figure 8 are those found by Knittle et al. (1986) for Fe-rich $MgSiO_3$ perovskite, as reported by Saxena et al. (1993) in a table labeled "$MgSiO_3$ perovskite," and those found by Mao et al. (1991) for an Fe-rich $MgSiO_3$ perovskite, as graphed by Chopelas (1996). In the lower sets of $\alpha(T)$ in Figure 8, the data are all for pure $MgSiO_3$ perovskite (with no Fe). On this basis, one should choose $\alpha(T)$ measured on a non Fe-bearing $MgSiO_3$ perovskite to calculate C_P and entropy for a non Fe-bearing $MgSiO_3$.

I note, however, the importance of the magnitude of $\alpha(T)$ in determining the composition of the lower mantle. Both Jackson (1983) and Jeanloz and Knittle (1989) emphasized that a large value of $\bar{\alpha}$ between 300 and 1700 K leads to a chondritic-like lower mantle, hence not a pyrolitic mantle composition. Zhao and Anderson (1994) showed that the α values reported by Mao et al. (1991), in contrast to the α data of Wang et al. (1994), lead to "drastic differences in the fraction of silicate perovskite in a two phase-mixture lower mantle."

The high value or the low value of $|(\partial K_T/\partial T)_P|$ for silicate perovskite?

The experimental values of $(\partial K_T/\partial T)_P$ vs. T are needed to find extrapolated values of the bulk modulus in this paper, in particular, column 4 of Table 3. This brings us squarely against the controversy about this parameter: Authors measuring this parameter are grouped just as in Figure 8. Those whose data on $\alpha(T)$ are in the upper set of Figure 8 also report a large value of $|(\partial K_T/\partial T)_P|$, where-

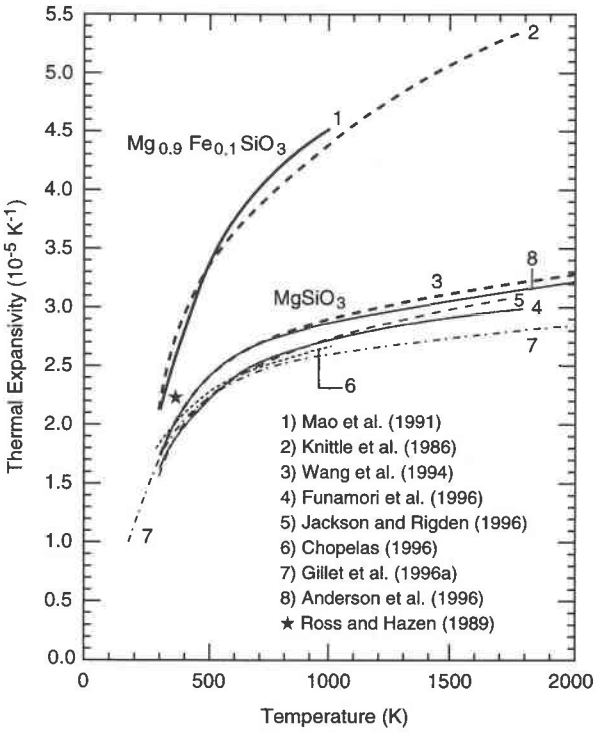

FIGURE 8. Thermal expansion, α, curves from experiments or the analysis of experiments. Note that the curves are sorted into two groups. The upper group of two curves shows a high value of α at high T. The lower group of six curves shows a much lower value of α at high T. The lower group represents the most current work. The lower group of $\alpha(T)$ curves results in $MgSiO_3$ having a larger density at lower mantle conditions than the lower mantle itself and thus favors a pyrolitic composition for the lower mantle. The upper group of $\alpha(T)$ curves yields a density at lower mantle conditions that, with little adjustment, matches the lower mantle density.

as those authors whose data occupy the lower sets have values about half as large (see Table 5).

The calculation of the $C_P - C_V$ correction and entropy requires an accurate value of K_T at high temperature, and to find K_T requires an accurate value of $(\partial K_T/\partial T)_P$ because measurements of K_S or K_T do not exist at high T. For $MgSiO_3$ perovskite, the values of $(\partial K_T/\partial T)_V$ are reported between −0.020 and −0.028 GPa/K, with the exception of the Stixrude et al. (1992) value, −0.060 GPa/K, on the basis of the Mao et al. (1991) data. I believe the value of $|(\partial K_T/\partial T)_P|$ reported by Stixrude et al. (1992) is much too high. If the Stixrude et al. value of $(\partial K_T/\partial T)_P = -0.06$ GPa/K is used, $K_T(T)$ of perovskite descends very rapidly with T, and, at temperatures corresponding to deep within the lower mantle, $K_T(T)$ of $MgSiO_3$ perovskite might approach $K_T(T)$ of MgO (see Fig. 9 of Anderson et al. 1996).

Even when neglecting the Stixrude et al. value, there is still a difference between values of $(\partial K_T/\partial T)_P$ listed in Table 5. I believe this is due to the fact that below the Debye temperature, the value of $|(\partial K_T/\partial T)_P|$ decreases

TABLE 5. High-temperature derivatives of the isothermal bulk modulus, K_T

Experimental reports	$(\partial K_T/\partial T)_P$ GPA K^{-1}
MgO	
Anderson et al. (1992)	−0.031
Al_2O_3	
Anderson et al. (1992)	−0.030
Mg_2SiO_4	
Anderson et al. (1992)	−0.023
Olivine	
Anderons et al. (1992)	−0.022
$MgSiO_3$ Perovskite	
Wang et al. (1994)	−0.023
Anderson and Masuda (1994)	−0.026
Utsumi et al. (1995)	−0.030
Funamori et al. (1996)	−0.028
Jackson and Rigden (1996) $T \approx 300$ K	−0.021
Jackson and Rigden (1996) $T > \Theta$	−0.028
Stixrude et al. (1992)	−0.060
Mao et al. (1991)	−0.063

steadily with decreasing T and eventually approaches zero at $T = 0$, similar to the behavior of C_P at T close to zero. I have used the graph showing $(\partial K_T/\partial T)_P$ over a wide temperature range presented by Jackson and Rigden (1996) as the basis for Figure 9, which is adapted from their Figure 6, to emphasize this point.

Authors whose data on α emphasize the lower temperatures report a lower value of $|(\partial K_T/\partial T)_P|$ than do the authors whose data emphasize the upper temperatures. I used the curves of $(\partial K_T/\partial T)_P$ and $(\partial K_S/\partial T)_P$ in Figure 9 to find by integration $K_T(T)$ and $K_S(T)$ from Yeganeh-Haeri's (1994) values of K_S and K_T at 300 K. The values so determined are listed in Tables 3 and 6.

ADDITIONAL THERMOELASTIC PROPERTIES OF $MgSiO_3$ PEROVSKITE

With the tabled values of K_T, K_S, as well as α available as a function of T, there are sufficient data for the determination of the Anderson-Grüneisen parameters,

$$\delta_T = -\left(\frac{1}{\alpha K_T}\right)\left(\frac{\partial K_T}{\partial T}\right)_P \tag{9}$$

and

$$\delta_S = -\left(\frac{1}{\alpha K_S}\right)\left(\frac{\partial K_S}{\partial T}\right)_P \tag{10}$$

The values of these parameters are listed in Table 6, columns 3 and 4. $K_0'(T)$ can be evaluated at 100 K intervals with the help of the value of $(\partial^2 K_T/\partial T \partial P)$, found by Jackson and Rigden (1996), 1.4×10^{-4} K^{-1}. Thus

$$K_0'(T) = K_0'(300) + 1.4 \times 10^{-4}(T - 300). \tag{11}$$

Values of T are listed in column 5, Table 6. The Grüneisen ratio, $\gamma = \alpha K_T V/C_V$, is next evaluated and listed in column 6 of Table 6.

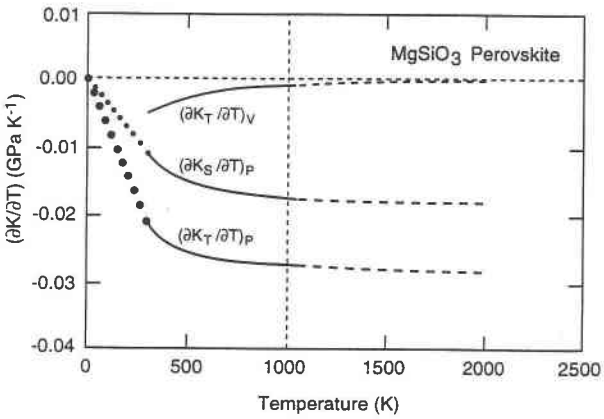

FIGURE 9. Values of the temperature derivatives of the bulk modulus vs. T for $MgSiO_3$ (modified from Fig. 6 of Jackson and Rigden 1996). Solid lines represent the range of available PVT data. Dashed lines represent extrapolations. Dotted lines represent the author's interpolation to absolute zero. It is to be noted that there is considerable variation in $(\partial K_S/\partial T)_P$ and $(\partial K_T/\partial T)_P$ between 300 K and about 800 K. It is also to be noted that $(\partial K_T/\partial T)_V$ approaches zero just beyond Θ.

The value of $q = (\partial \ln\gamma/\partial \ln V)$ can be evaluated from the equation (Anderson 1995).

$$q = \delta_T - K' + 1\left(\frac{\partial \ln C_v}{\partial \ln V}\right)_T. \qquad (12)$$

At $T > \Theta$, the $(\partial \ln C_v/\partial \ln V)$ term vanishes, so that for $T \approx \Theta$, Table 6 shows that δ_T is close to K_0', and thus q is very close to unity.

The value of v_s is determined from Θ_D^{ac} by means of Equations 3 and 4 and v_b from K_S and ρ, where K_S comes primarily from the Jackson and Rigden (1996) determination of $(\partial K_S/\partial T)_P$, and ρ comes from the Funamori et al. (1996) data on $V(T)$. Through v_b and v_s, v_p is determined by $v_p^2 = K/\rho + 4/3\ v_s^2$. The variation of Poisson's ratio with T is calculated from v_s and K/ρ. It is seen from Table 7 that σ varies between 0.224 and 0.238 from 300 to 1800 K, similar to the variation of σ in Al_2O_3 (Anderson and Isaak 1995). The value of the isotropic shear modulus, determined from $G = \rho\ v_s^2$, is listed in Table 7.

THERMAL PRESSURE IN THE EQUATION OF STATE

In PVT calculations where a thermal equation of state is used, the contribution to temperature effects comes from the thermal pressure, ΔP_{Th}. At high T in the quasiharmonic approximation, P_{Th} is proportional to T, and the proportionality parameter is αK_T (Anderson 1995).

The equation to obtain the thermal pressure using αK_T (Anderson and Zou 1989), where P_{Th} is a function of V and T, is

$$\Delta P_{TH} = \alpha K_T(T - T_0) - (\partial K_T/\partial V)_v \ln\frac{V}{V_0}. \qquad (13)$$

Jackson and Rigden (1996) correctly pointed out that to obtain ΔP_{Th} in P-T space, Equation 13 is not rigorously correct because of the omission of a small correction term, resulting from going from V-T space to P-T space. This term is $(\alpha K_T/\partial T)_V \int_{T_0}^{T}\int_{T_0}^{T} \alpha dT\, dT$. Jackson and Rigden (1996) in fact show in their Figure 6 that $(\partial K_T/\partial T)_V$ is vanishingly small for $T = \Theta$ and higher temperatures for $MgSiO_3$ perovskite (see also Fig. 9 of this report). It is a fraction of a percent between 300 and Θ. The double integral term is large at high T, but it is severely depressed by the smallness of $(\alpha K_T/\partial T)_V$ at high T. At low T, where $(\partial K_T/\partial T)_V$ is just a few percent, the double integral term is small because of the value of α and the smallness of T. The correction term was evaluated at all temperatures and found to be insignificant in the calculation of ΔP_{Th}, so that Equation 13 is sufficient even though it is not rigorous.

The value of ΔP_{Th} at 1800 K is 10 GPa for $MgSiO_3$ perovskite (Table 6). This is to be compared with $\Delta P_{Th}(1800) = 9.24$ for Al_2O_3 (Anderson and Isaak 1995), a value consistent with the change of ρ_0 for the two solids. According to quasiharmonic theory, in the high-T approximation, the value of $\overline{\alpha K_T}$, which is the coefficient defined by $(\partial P_{Th}/\partial T)_V$, of silicates with an average mass of 20–21, should increase from mineral to mineral as $\Theta^{4/3}$ (Anderson 1995). The increase in $\Theta^{4/3}$ from Al_2O_3 to $MgSiO_3$ perovskite is 5.5%; the increase in the high-T value of αK_T is about 5%. This means that the ΔP_{Th}-T relationship of $MgSiO_3$ perovskite fits nicely into the pattern of ΔP_{Th} vs. T of rock-forming minerals (Fig. 2.3 in Anderson 1995). This constitutes a cross check on the value of αK_T at high T.

TABLE 6. Dimensionless thermoelastic parameters and thermal pressure parameters for $MgSiO_3$ perovskite, arising from the Debye model

T (K)	K_S* Adiabatic bulk mod. (GPa)	δ_T†	δ_S‡	K_0'§	γ#	q^	αK_T‖ (MPa)	ΔP_{TH}** Thermal pressure (GPa)
300	264.0			4.00	1.52		4.38	0
400	262.8	4.98	4.14	4.014	1.41	(1.39)	5.13	0.47
500	262.0	4.87	3.94	4.028	1.37	(1.34)	5.62	1.015
600	260.7	4.78	3.92	4.042	1.39	(1.34)	6.03	1.597
700	259.2	4.65	3.84	4.056	1.38	(1.29)	6.24	2.210
800	258.0	4.40	3.81	4.076	1.40	(1.12)	6.46	2.846
900	256.9	4.23	3.77	4.084	1.40	(1.05)	6.59	3.505
1000	254.2	4.09	3.85	4.098	1.39	0.97	6.66	4.168
1100	252.4	4.06	3.87	4.112	1.40	0.95	6.68	4.835
1200	250.2	4.05	3.81	4.126	1.40	0.93	6.71	5.504
1300	248.7	4.04	3.83	4.140	1.40	0.90	6.73	6.175
1400	246.9	4.03	3.84	4.154	1.38	0.88	6.74	6.848
1500	245.1	4.03	3.86	4.168	1.40	0.86	6.75	7.522
1600	243.2	4.03	3.86	4.182	1.40	0.85	6.76	8.198
1700	241.4	4.03	3.86	4.196	1.40	0.83	6.77	8.874
1800	239.5	4.03	3.86	4.210	1.41	0.82	6.78	9.951

*K_S at 300 K from Yeganeh-Haeri (1994).
†$\delta_T = -(1/\alpha K_T)(\partial K_T/\partial T)_P$.
‡$\delta_S = -(1/\alpha K_S)(\partial K_S/\partial T)P$.
§$K_0'(T) = K_0' + 1.4 \times 10^{-4}(T - 300)$.
#$\gamma = \alpha K_T V/C_V$.
‖$q(T) = \delta_T - K_0'(T) + 1$ above $T = \Theta$.
**$\Delta P_{TH} = P_{TH}(T) - P_{TH}(300)$.

TABLE 7. Isotropic sound velocities and Poisson's ratio

T (K^{-1})	ρ^* (g/cm³)	v_m† (km/s)	v_s‡ (km/s)	v_b§ (km/s)	v_p# (km/s)	σ‖	G** (GPa)
300	4.104	7.272	6.57	8.00	11.04	0.224	177
400	4.094	7.230	6.53	7.97	10.97	0.226	175
500	4.087	7.187	6.49	7.94	10.92	0.227	172
600	4.084	7.142	6.45	7.91	10.86	0.228	170
700	4.068	7.104	6.41	7.88	10.82	0.229	167
800	4.051	7.066	6.38	7.86	10.77	0.230	165
900	4.045	7.022	6.34	7.82	10.71	0.231	163
1000	4.035	6.980	6.30	7.79	10.66	0.232	160
1100	4.028	6.936	6.26	7.75	10.60	0.232	158
1200	4.009	6.900	6.23	7.73	10.56	0.233	155
1300	3.993	6.861	6.19	7.70	10.51	0.234	153
1400	3.982	6.820	6.15	7.67	10.45	0.235	151
1500	3.971	6.778	6.12	7.63	10.39	0.235	149
1600	3.958	6.737	6.08	7.60	10.34	0.236	146
1700	3.951	6.694	6.04	7.56	10.28	0.237	144
1800	3.938	6.653	6.00	7.52	10.23	0.238	142

*Calculated from V (Table 3, column 5).
†Calculated from Θ_D^{ac} in Table 2 and Equations 3 and 5.
‡Calculated from Equation 5.
§Calculated from $\sqrt{K_S/\rho}$; K_S from Table 6.
#Calculated from $v_p^2 = (K_S/\rho) + (4/3)v_s^2$.
‖Calculated from v_s and v_p above. $\sigma = [(v_p^2/v_s^2) - 2]/\{2[(v_p^2/v_s^2) - 1]\}$.
**G calculated from $G = \rho v_s^2$.

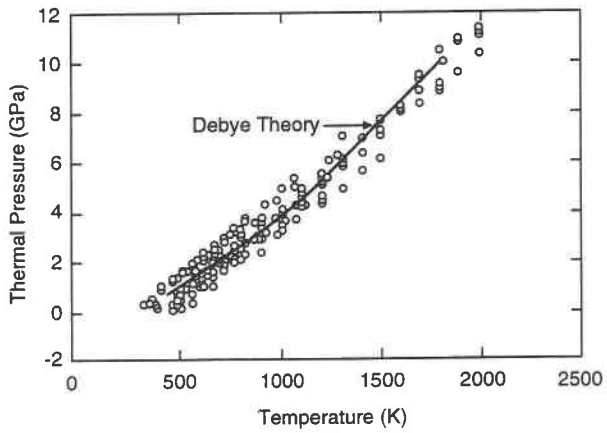

FIGURE 10. Thermal pressure vs. temperature for $MgSiO_3$ perovskite. The circles represent the database presented by Jackson and Rigden (1996), who analyzed experimental data from four reports. The solid line represents thermal pressure values found from the Debye model (Table 6) (figure adapted from Fig. 5a of Jackson and Rigden 1996).

Using Equation 13, Jackson and Rigden (1996) analyzed the *PVT* data of $MgSiO_3$ perovskite from four experiments (Ross and Hazen 1989; Wang et al. 1994; Utsumi et al. 1995; Funamori et al. 1996) and found thermal pressure vs. T. The variation of ΔP_{Th} vs. T is shown by small circles in Figure 10, which is modified from Figure 5a of Jackson and Rigden (1996). Also plotted in this figure as a solid line is ΔP_{Th} obtained in this study (listed in the last column of Table 6). In Figure 10, we observe that the calculated Debye value of ΔP_{Th}, found in Table 6, is in agreement with that obtained from experiment, which means that for $MgSiO_3$ perovskite, the Debye model produces a satisfactory equation of state. In addition, when Equation 13 was replaced by the Mie-Grüneisen term for thermal pressure,

$$\Delta P_{TH} = \left(\frac{\gamma}{V}\right)[E_{Th}(T) - E_{Th}(T_0)] \qquad (14)$$

(see Fig. 5b of Jackson and Rigden 1996), satisfactory agreement with experiment was also found.

CROSS CHECKS AND COMPARISON WITH OTHER REPORTS

K_S

K_S was determined from the curve of $(\partial K_S/\partial T)_P$ vs. T as taken from Jackson and Rigden's (1996) Figure 9. K_S could also have been calculated from $K_S = K_T(C_P/C_V)$, but I used this equation as a cross check. From Tables 2 and 4, at 1000 K, $K_T(C_P/C_V) = 255.4$, and from Table 6, as determined from Jackson and Rigden's (1996) $(\partial K_S/\partial T)_P$, $K_S = 254.2$, off by 0.4%. The difference is 0.07% at 500 K. This cross check also constitutes a verification of the Jackson and Rigden (1996) calculations of $K_S(T)$ and $(\partial K_S/\partial T)_P$.

δ_T

I obtain $\delta_T = 5.0$ at 300 K and 4.03 at $T \geq \Theta$. The steady change in δ_T from $300 < T < 1000$ and the constancy of δ_T for $T > \Theta$ agree well with what has been found for MgO, Al_2O_3, and Mg_2SiO_4 (Anderson and Isaak 1995) (Fig. 11). The value, $\gamma_0 = 1.5$ at 300 K, was found by Anderson et al. (1995a) in the comparison of isentropes of ρ vs. P for $MgSiO_3$ perovskite and the adiabat of the mantle, and $\gamma_0 = 1.3$ at room temperature has also been reported by Gillet et al. (1996a). $\delta_{T_0} = 5$ agrees reasonably well with the ambient measurements of Chopelas (1996), 4.3, who made spectroscopic measurements in the diamond cell. For measurements taken over a range of temperatures from 300 K upward, δ_{T_0} should be lower than 5. Thus my results are consistent with the value determined by Anderson et al. (1996), 4.5, from the room-pressure, high-temperature measurement of Utsumi et al. (1995), 4.5, the Wang et al. (1994) value measured at 4.3, and the value 4.2 of Gillet et al. (1996a). At variance with this data is the report of Stixrude et al. (1992) that $\delta_T \approx 7$.

The value of δ_T enables one to compute the value of α at high pressure using the definition of $\delta_T = -(\partial \ln \alpha/\partial \ln \rho)_T$, which upon integration becomes

$$\left(\frac{\alpha}{\alpha_0}\right) = \left(\frac{\rho}{\rho_0}\right)^{-\delta_T}. \qquad (15)$$

Let us find α at the conditions, $P = 125$ GPa and 2500 K, where Gillet et al. (1996a) reported $\alpha = 1.1 \times 10^{-5}$ K^{-1}. At these conditions, $\rho/\rho_0 = 5.49/4.08 = 1.345$. The value of δ_T at high T is 4.03, according to Table 6, and α_0 from the Gillet et al. (1996a) data (see Fig. 8) at 2500 K (P = 0) is 3.0×10^{-5} K^{-1}. From Equation 15, $\alpha = 0.88 \times 10^{-5}$ K^{-1}, which is below the Gillet et al. value. If we further consider the variation of δ_T with volume,

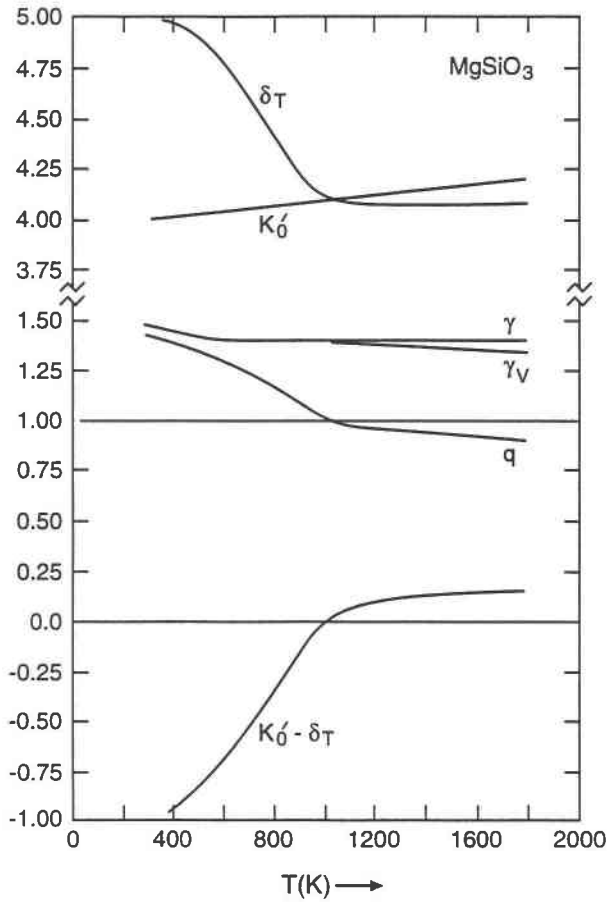

FIGURE 11. Plots of δ_T and δ_S vs. T for $MgSiO_3$ perovskite, $\gamma = \alpha K_T V/C_V$, and γ_V vs. T (all determined in this report). $q = \delta_T - K_0' + 1 + (\partial \ln C_V/\partial \ln V)_T$ and $K_0' - \delta_T$ are plotted. $q = \delta_T - K_0' + 1 + (\partial \ln C_V/\partial \ln V)_T$ shows that $q = 1$ at $T = 1000$ K and is close to unity elsewhere. The plot of $K_0' - \delta_T$ shows its resemblance to $(\partial K_T/\partial T)_V$ in Figure 9.

the predicted α is somewhat higher. Anderson and Isaak (1993) recommended that δ_T change with (ρ/ρ_0) as $\delta_T = \delta_{T_0}(\rho_0/\rho)^\kappa$; when placed in Equation 15, the aforementioned equation for δ_T gives

$$\frac{\alpha}{\alpha_0} = \exp\left\{-\frac{\delta_{T_0}}{\kappa}\left[1 - \left(\frac{\rho_0^\kappa}{\rho}\right)\right]\right\} \quad (16)$$

(Anderson and Isaak 1993). Anderson and Isaak (1993) found $\kappa = 1.5$ for MgO, which agrees with the report by Gillet et al. (1996a) that ambient δ_T decreases to 3.5 at 100 GPa. Using $(\rho_0/\rho) = 0.740$ corresponding to 125 GPa, $\kappa = 1.5$, and the high-T value 4.04 for δ_T, $\alpha = 0.37\alpha_0$ or $\alpha = 1.11 \times 10^{-5}$ K^{-1}. This is a good match with the Gillet et al. (1996a) data point; I regard it as a satisfactory cross check on the value of δ_T at high T, 4.03, found in this report. Using the value of δ_T presented by Stixrude et al. (1992), $\delta_T = 7$, the value of α at 125 GPa and 2500 K would by Equation 15 and by Equation 16 be unreasonably low.

γ

The steady descent of γ from 300 to 800 K and the subsequent value at high T being independent of T are consistent with the $\gamma(T)$ behavior of other dense oxides (Anderson and Isaak 1995). The $T = 300$ K value of γ found here, 1.52, is consistent with previous estimates that involved the author (Anderson and Masuda 1994; Anderson et al. 1995a). This is to be compared with the Chopelas (1996) value, 1.42, found from spectroscopic measurements in a diamond cell. At high T, the value of γ reported here is 1.4 and $(\partial\gamma/\partial T)_P = 0$. This value of γ is reasonably close to the high-temperature values of Wang et al. (1994) and Gillet et al. (1996a), who both found $\gamma = 1.3$ from their measurements. Jackson and Rigden (1996) found $\gamma = 1.33$ at high T. The Utsumi et al. (1995) data on $V(T)$ lead to $\gamma = 1.45$, according to the analysis of Masuda and Anderson (1995). Stacey (1996) found $\gamma = 1.30 \pm 0.09$ for the high-T (2000 K) value of the perovskite structure by the classical method (displacement on pairs of neighboring atoms in the lattice is summed to obtain the net force and the resultant force is made equal to the thermal pressure).

There is, of course, the report by Hemley et al. (1992) that $\gamma = 1.96(9)$, which is at variance with the other reports listed above. It is conceivable that γ would be larger for an Fe-rich perovskite than for pure perovskite, but according to Anderson et al. (1996) a thermodynamic constraint prevents γ from being greater than $0.5\ K_0' - 0.3$. The Hemley et al. (1992) reported value of $K_0' = 3.9$ requires that $\gamma < 1.6$; thus $\gamma = 1.96(9)$ appears inconsistent with $K_0' = 3.9$.

The Jackson and Rigden (1996) value of γ, 1.33, determined from a Mie-Grüneisen fit to the *PVT* data, is slightly less than that shown in Table 6, 1.40 at $T = \Theta$, which was calculated directly from α and K_T through the definition, $\gamma = \alpha K_T V/C_V$, but this can be considered as good agreement.

q

As shown in Table 6 and Figure 7, the value of q is near unity and is exactly unity at 1000 K. Jackson and Rigden (1996) suggested that other properties are not sensitive to the exact value of q, so that $q = 1$ was assumed. In this report I find that near $T = \Theta$, $q = 1$ is exact. Gillet et al. (1996a) found $q = 1$, but Hemley et al. (1992) reported $q = 2.5(1.7)$. Cynn et al. (1996) found that for Mg_2SiO_4, $(\partial \ln C_V/\partial \ln V)$ rises steadily from 0 to 1 as T decreases from Θ to 0. Using a straight line for interpolation, the values of $(\partial \ln C_V/\partial \ln V)_T$ between $0 < T < 1000$ were obtained, giving the values of q to be used in Equation 12 at low T. The values of q obtained using the interpolated values of $(\partial \ln C_V/\partial \ln V)_T$ are shown in the parentheses of column 7, Table 6 (see Bina 1995 for a discussion of the uncertainty in q from previous studies).

$(\partial K_T/\partial T)_V$

A plot of this parameter vs. T, determined by Jackson and Rigden (1996), is shown in Figure 9. $(\partial K_T/\partial T)_V$ can

also be determined by the data in Table 6 through the thermodynamic identity,

$$\left(\frac{\partial K_T}{\partial T}\right)_V \equiv \alpha K_T(K_0' - \delta_T) \quad (17)$$

(see Anderson 1995, p. 57–58). Because αK_T does not change significantly with T (neglecting the values at 400 K and 500 K), $(\partial K_T/\partial T)_V$ should vary as $K_0' - \delta_T$, which is plotted on the bottom of Figure 11. The resemblance between the curve $(K_0' - \delta_T)$ determined in this report and $(\partial K_T/\partial T)_V$ determined by Jackson and Rigden (1996) (Fig. 9) constitutes a cross check on the values of δ_T. The value of $K_0' - \delta_T$ vs. T from the curve in Figure 11 and the data for αK_T in Table 6 yield, by Equation 17, $(\partial K_T/\partial T)_V = -0.0044$ GPa/K at 300 K, whereas Jackson and Rigden (1996) reported $(\partial K_T/\partial T)_V = -0.005$ GPa/K at ambient conditions. This excellent agreement constitutes a cross check on $(\partial K_T/\partial T)_V$ as determined in this study.

$(\partial P_{Th}/\partial V)_T$

Because of the identity $(\partial K_T/\partial T) \equiv -V[\partial(\alpha K_T)/\partial V]_T$, $[(\partial \alpha K_T)/\partial V]_T$ vanishes when $K_0' - \delta_T = 0$. But P_{Th} is proportional to T, and $(\partial P_{Th}/\partial T)_P = \alpha K_T$, so $(\partial P_{Th}/\partial V)_T$ also vanishes when $\delta_T - K_0'$ vanishes (Anderson et al. 1992; Masuda and Anderson 1995). Anderson et al. (1995b) showed from a study on MgO that when $\delta_T - K_0' = \pm 0.2$, the thermal pressure is, for all practical purposes, independent of volume. Figure 11 shows that from about 900 K up to 1800 K, $K_0' - \delta_T < |0.2|$, so the thermal pressure of $MgSiO_3$ perovskite is independent of volume at high T. In this regard $MgSiO_3$ perovskite is like Al_2O_3 and MgO (Anderson 1997). However, the value of the width of the volume zone necessary to satisfy $(\partial P_{Th}/\partial V)_T = 0$ is not apparent. Nevertheless for high temperatures it appears that one could safely assume that for a reasonably wide compression range, say for V/V_0 between 1 and 0.9, the thermal pressure, $P_{Th}(V_0,T)$, depends only on T, not on V. This means that the upper part of the curve in Figure 10 does not shift as the volume is changed.

Conclusions

It is shown that $MgSiO_3$ perovskite is a Debye-like solid because the specific heat and entropy calculated to high T (1800 K) from Debye theory agree with available experimental data, especially those above 400 K. In this calculation, the thermal expansivity data of Funamori et al. (1996) and the acoustic velocity data of Yeganeh-Haeri (1994) are used as input. It is also shown that a number of thermoelastic properties, including $(\partial K_T/\partial T)_P$, $(\partial K_T/\partial T)_V$, K_T, K_S, δ_T, δ_S, γ, q, v_s, v_p, and G, can be calculated and tabled up to high T once it has been proved that $MgSiO_3$ perovskite is a Debye-like solid. From the calculated properties, K_T, K_S, γ, ρ, and $(\partial K_T/\partial T)_V$, the thermal pressure, ΔP_{Th}, can also be calculated to high T. When this is done, the resulting values of ΔP_{Th} are shown to agree with ΔP_{Th} calculated by Jackson and Rigden (1996) from the existing PVT data set. Thus for $MgSiO_3$ perovskite, Debye theory can be used to obtain the equation of state.

$MgSiO_3$ perovskite joins a small group of Debye-like minerals, now consisting of: MgO, Al_2O_3, and $MgSiO_3$ perovskite. For this group, the physical properties described above are calculated from data on acoustic sound velocities, ignoring the optic properties. The criterion for selection as a Debye-like solid is that the majority of optic modes occur at frequencies placed toward the center of the phonon density of states, e.g., the Debye frequency is larger in value than the frequencies of the majority of optic modes. By this criterion, other dense minerals, such as stishovite and $MgSiO_3$ ilmenite, are not likely candidates to be Debye-like solids.

Olivine is a near Debye-like solid. Guyot et al. (1996) showed that although Debye theory gives values close to experiment for the properties of C_V, S, and ΔP_{Th} in olivine, the Kieffer approximation to the density of states gives values even closer to experiment.

Acknowledgments

The author acknowledges helpful conversations on several topics in this paper with Ann Chopelas, François Guyot, Guillaume Fiquet, Lars Stixrude, Russ Hemley, and Ian Jackson. I thank Philippe Gillet for editorial assistance and helpful comments on a previous version of this paper. John Carnes assisted with calculations on C_p and S. Overall calculations were checked by Judy Hohl using a spreadsheet. Supported by NSF grant EAR-96-14654. Support by ONR acknowledged. IGPP no. 4853.

References cited

Akaogi, M. and Ito, E. (1993) $MgSiO_3$ perovskite. Geophysical Research Letters, 20, 105–108.

Anderson, O.L. (1963) A simplified method of calculating the Debye temperature from elastic constants. Journal of Physics and Chemistry of Solids, 24, 909–917.

———(1995) Equations of state of solids for geophysics and ceramic science. Oxford University Press, New York.

———(1997) The volume dependence of the thermal pressure of solids. Journal of Physics and Chemistry of Solids, 58, 335–343.

Anderson, O.L. and Isaak, D.G. (1993) The dependence of the Anderson-Grüneisen parameter, δ_T, upon compression at extreme conditions. Journal of Physics and Chemistry of Solids, 54, 221–227.

———(1995) Elastic constants of mantle minerals at high temperatures. In T.J. Ahrens, Ed., Mineral physics and crystallography: A handbook of physical constants (Reference Shelf 2), p. 64–97. American Geophysical Union, Washington, D.C.

Anderson, O.L. and Masuda, K. (1994) A thermoelastic method for computing thermal expansivity, α, vs. T along isobars for silicate perovskite. Physics of the Earth and Planetary Interiors, 85, 227–236.

Anderson, O.L. and Zou, K. (1989) Formulation of the thermodynamic functions for mantle minerals: MgO as an example. Journal of Physics and Chemistry of Minerals, 16, 642–648.

Anderson, O.L., Isaak, D., and Oda, H. (1992) High-temperature elastic constant data on minerals relevant to geophysics. Reviews of Geophysics, 30, 57–90.

Anderson, O.L., Masuda, K., and Guo, D. (1995a) Pure silicate perovskite and the PREM lower mantle model: A thermodynamic analysis. Physics of the Earth and Planetary Interiors, 89, 33–49.

Anderson, O.L., Masuda, K., and Isaak, D.G. (1995b) A new thermodynamic approach for high-pressure physics. Physics of the Earth and Planetary Interiors, 91, 3–16.

———(1996) Limits on the value of δ_T and γ for $MgSiO_3$ perovskite. Physics of the Earth and Planetary Interiors, 98, 31–46.

Barron, T.H.K. (1955) Thermal expansion of solids at low temperatures. Philosophical Magazine, 7, 720–727.

———(1957) Grüneisen parameters for the equation of state of solids. Annals of Physics, 1, 77–89.
———(1977) Room temperature Debye-Waller factors of magnesium oxide. Acta Crystallography, A33, 602–604.
Barron, T.H.K., Collins, J.G., and White, G.K. (1980) Thermal expansion of solids at low temperatures. Advances in Physics, 29, 609–730.
Bina, C.R. (1995) Confidence limits for silicate perovskite equations of state. Physics and Chemistry of Minerals, 22, 375–382.
Birman, J.L. (1984) Theory of crystal space groups and lattice dynamics, 538 p. Springer-Verlag, Berlin.
Born, M. (1915) Dynamik der Kristallgitter, 1st Ed. Tuebner Press, Leipzig.
———(1923) Atomtheorie der festen Zustandes, 2nd Ed. Tuebner Press, Leipzig.
Chopelas, A. (1990) Thermal expansion, heat capacity, and entropy of MgO at mantle pressure. Physics and Chemistry of Minerals, 17, 142–148.
———(1996) Thermal expansivity of lower mantle phase of MgO and $MgSiO_3$ perovskite at high pressure, derived from spectroscopy. Physics of the Earth and Planetary Interiors, 98, 3–16.
Chopelas, A., Boehler, R., and Ko, T. (1994) Thermodynamics and behavior of γ-Mg_2SiO_4 at high pressure: Implications for Mg_2SiO_4 phase equilibrium. Physics and Chemistry of Minerals, 21, 351–359.
Choudhury, N., Chapalet, S.L., Rao, K.R., and Ghose, S. (1988) Lattice dynamics of $MgSiO_3$ perovskite. Pramāna Journal of Physics, 30, 423–428.
Cynn, H., Carnes, J.D., and Anderson, O.L. (1996) Thermal properties of forsterite, including C_V, calculated from αK_T through the entropy. Journal of Physics and Chemistry of Solids, 11, 1593–1599.
Debye, P. (1912) Zur Theorie der spezifischen Wärmen. Annalen der Physik, 39, 789.
Funamori, N., Yagi, T., Utsumi, W., Kondo, T., and Uchida, T. (1996) Thermoelastic properties of $MgSiO_3$ perovskite determined by in situ x-ray observations up to 30 GPa and 2000 K. Journal of Geophysical Research, 101, 8257–8269.
Gillet, P. (1996) Raman spectroscopy at high pressure and high temperature. Phase transitions and thermodynamic properties of minerals. Physics and Chemistry of Minerals, 23, 263–265.
Gillet, P., Guyot, F., Price, G.D., Tournerie, B., and Le Cleach, A. (1993) Phase changes and thermodynamic properties of $CaTiO_3$: Spectroscopic data, vibrational modelling and some insights on the properties of $MgSiO_3$ perovskite. Physics and Chemistry of Minerals, 20, 159–170.
Gillet, P., Guyot, F., and Wang, Y. (1996a) Microscopic anharmonicity and equation of state of $MgSiO_3$–perovskite. Geophysical Research Letters, 23, 3043–3046.
Gillet, P., McMillan, P., Schott, J., Badro, J., and Grzechnik, A. (1996b) Thermodynamic properties and isotopic fractionation of calcite from vibrational spectroscopy of ^{18}O-substituted calcite. Geochimica Cosmochimica Acta, 60, 3471–3485.
Guyot, F., Wang, Y., Gillet, P., and Ricard, Y. (1996) Quasi-harmonic computations of thermodynamic parameters of olivines at high-pressure and high-temperature. A comparison with experiment data. Physics of the Earth and Planetary Interiors, 98, 17–29.
Hemley, R.J., Stixrude, L., Fei, Y., and Mao, H.K. (1992) Elasticity and equation of state of perovskite: Implications for the earth's lower mantle. In Y. Syono and M.H. Manghnani, Eds., High pressure research: Applications to earth and planetary sciences, p. 183–190. American Geophysical Union, Washington, D.C.
Jackson, I. (1983) Some geophysical constraints on the chemical composition of the Earth's lower mantle. Earth and Planetary Science Letters, 62, 91–103.
Jackson, I. and Rigden, S.M. (1996) Analysis of *P-V-T* data: Constraints on the thermoelastic properties of high-pressure minerals. Physics of the Earth and Planetary Interiors, 96, 95–112.
Jeanloz, R. and Knittle, E. (1989) Composition of the lower mantle. Philosophical Transactions of the Royal Society of London A, 328, 377–389.
Kieffer, S.W. (1982) Thermodynamics and lattice vibrations of minerals: 5. Applications to phase equilibria, isotopic fractionation, and high-pressure thermodynamic properties. Reviews of Geophysics and Space Physics, 20, 827–849.
———(1985) Heat capacity and entropy. In Mineralogical Society of America Reviews in Mineralogy, 14, 65–126.
Kittel, C. (1971) Introduction to solid state physics (4th edition), 617 p. Wiley, New York.
Knittle, E., Jeanloz, R., and Smith, G.L. (1986) The thermal expansion of silicate perovskite and stratification of the Earth's mantle. Nature, 319, 214–216.
Liebermann, R.C. (1982) Elasticity of minerals at high pressure and temperature. In W. Schreyer, Ed., High pressure researches in geosciences, p. 1–14. Schweizerbart'sche, Stuttgart.
Lu, R., Hofmeister, A.M., and Wang, Y. (1994) Thermodynamic properties of ferromagnesium silicate perovskites from vibrational spectroscopy. Journal of Geophysical Research, 99, 11,795–11,804.
Mao, H.K., Hemley, R.J., Fei, Y., Shu, J.F., Chen, L.C., Jephcoat, A.P., Wu, Y., and Bassett, W.A. (1991) Effect of pressure, temperature and composition on lattice parameters and density of $(Fe,Mg)SiO_3$ perovskite to 30 GPa. Journal of Geophysical Research, 96, 8069–8079.
Masuda, K. and Anderson, O.L. (1995) The isentropic density profile of perovskite computed by the thermal pressure. Geophysical Research Letters, 22, 2211–2214.
Navrotsky, A. (1989) Thermochemistry of perovskites. In A. Navrotsky and D.J. Weidner, Eds., Perovskite: A structure of great interest to geophysics and materials science, p. 67–80. Geophysics Monograph 45, American Geophysical Union, Washington, D.C.
Poirier, J.P. (1991) Introduction to the physics of the earth's interior, 261 p. Cambridge University Press, Cambridge.
Ross, N.L., and Hazen, R.M. (1989) Single crystal x-ray diffraction study of $MgSiO_3$ perovskite from 77 to 400 K. Physics and Chemistry of Minerals, 16, 415–420.
Sangster, M.J.L., Peckham, G., and Saunderson, D.H. (1970) Lattice dynamics of magnesium oxide. Journal of Physical Chemistry, 3, 1026–1036.
Saxena, S.K., Chatterjee, N., Fei, Y., and Shen, G. (1993) Thermodynamic data on oxides and silicates, 297 p. Springer-Verlag, Berlin, Heidelberg.
Shankland, T.J. (1972) Velocity-density systematics: Derivation from Debye theory and the effect of ionic size. Journal of Geophysical Research, 77, 3750–3758.
Stacey, F.D. (1996) Thermoelasticity of $(Mg,Fe)SiO_3$ perovskite and a comparison with the lower mantle. Physics of the Earth and Planetary Interiors, 98, 65–78.
Stixrude, L., Hemley, R.J., Fei, Y., and Mao, H.K. (1992) Thermoelasticity of silicate perovskite and magnesiowüstite and stratification of the earth's mantle. Science, 257, 1099–1101.
Utsumi, W., Funamori, N., Yagi, T., Ito, E., Kikegawa, T., and Shimomura, O. (1995) Thermal expansivity of $MgSiO_3$ perovskite under high pressures up to 20 GPa. Geophysical Research Letters, 22, 1005–1008.
Wang, Y., Weidner, D.J., Liebermann, R.C., and Zhao, Y. (1994) *P-V-T* equation of state of $(Mg,Fe)SiO_3$ perovskite: Constraints on composition of the lower mantle. Physics of the Earth and Planetary Interiors, 83, 13–40.
White, G.K. and Anderson, O.L. (1966) Grüneisen parameter for magnesium oxide. Journal of Applied Physics, 430–433.
Winkler, B. and Dove, M.T. (1992) Thermodynamic properties of $MgSiO_3$ perovskite derived from large scale molecular motions. Physics and Chemistry of Minerals, 18, 407–415.
Yeganeh-Haeri, A. (1994) Synthesis and reinvestigation of the elastic properties of single crystal magnesium silicate perovskite. Physics of the Earth and Planetary Interiors, 87, 111–121.
Zhao, Y. and Anderson, D.L. (1994) Mineral constraints on the chemical composition of the Earth's lower mantle. Physics of the Earth and Planetary Interiors, 85, 273–292.

MANUSCRIPT RECEIVED MARCH 18, 1997
MANUSCRIPT ACCEPTED AUGUST 22, 1997